

8-D Reflectance Field for Computational Photography

Seiichi Tagawa

Yasuhiro Mukaigawa
ISIR, Osaka University, Japan
tagawa@am.sanken.osaka-u.ac.jp

Yasushi Yagi

Abstract

Some computational photography techniques have been proposed to control the focus and illumination of captured images. However, the relationship between the techniques have been unclear because they were developed independently for different purposes. In this research we propose a unified framework to explain the computational photography techniques in the computation of an 8-D reflectance field. Moreover, for an 8-D reflectance field we show that the synthetic aperture, the image-based relighting, and the confocal imaging techniques can be realized using the same measuring device.

1. Introduction

We often want to change the focusing or illumination conditions of photographs after they are captured, hence, some computational photography techniques have been proposed. For refocusing, the synthetic aperture [9] can tighten the depth-of-field or shift the focal plane. For relighting, the Light Stage[2] can generate images of the target object under arbitrary illumination conditions. Moreover, by controlling both focus and illumination, the confocal imaging[6] can clearly visualize a particular depth

The formulation and the implementation of these computational photography techniques are optimized to a specific situation because they are specialized for different purposes in different research fields. Hence, the relationship between them has been unclear.

In this paper, we introduce a unified framework to explain computational photography techniques based on an 8-D reflectance field (8DRF). The 8DRF represents the relationship between 4-D illumination and 4-D observation light fields. Since the 8DRF includes all information about illumination and reflection, the synthetic aperture, the image-based relighting, and the confocal imaging techniques can be explained as a computation of the 8DRF in the proposed framework. To confirm the validity of our framework, we have imple-

mented these computational photography techniques on one system using the Turtleback Reflector[7], which is only one device for sampling an 8DRF over a hemisphere at uniform intervals.

2. Reflectance Field

2.1. Definition of an 8-D Reflectance Field

The image of a scene varies when the viewpoint or the illumination changes. It is well known that these appearances can be perfectly represented by a set of rays in a scene.

First, we consider reflected rays from the scene. A ray can be expressed by the passing point (x, y, z) in the direction (θ, ϕ) as shown in Fig.1(a). Hence, the intensity of the ray can be defined by five parameters. This description of the rays is called the *light field*. Here, assuming the ray is not attenuated in the scene, the intensity of the ray can be defined by four parameters (s, t) and (u, v) on two planes as shown in Fig.1(b). While this is a standard representation, it cannot describe rays that are parallel to the two planes. Hence, in this research we define the light field using a hemisphere which covers the scene as shown in Fig.1(c). The ray is denoted by the position on the hemisphere $\mathbf{D}_R = (\theta_R, \phi_R)$ and the direction $\mathbf{C}_R = (u_R, v_R)$. This is a four dimensional light field (4DLF) denoted by $F_R(\mathbf{D}_R, \mathbf{C}_R)$ which can represent all the reflected rays from the scene.

Similarly, the illumination to the scene is also described as a light field. As shown in Fig.1(d), the incident ray can be defined by the position on the hemisphere $\mathbf{D}_L = (\theta_L, \phi_L)$ and the direction $\mathbf{C}_L = (u_L, v_L)$. Hence, we can denote the 4DLF of the illumination by $F_L(\mathbf{D}_L, \mathbf{C}_L)$.

The relationship between the 4DLF of the illumination F_L and the 4DLF of the reflection F_R is called the *reflectance field*. Hence, we can denote the reflectance field with eight parameters by:

$$F(\mathbf{D}_L, \mathbf{C}_L, \mathbf{D}_R, \mathbf{C}_R), \quad (1)$$

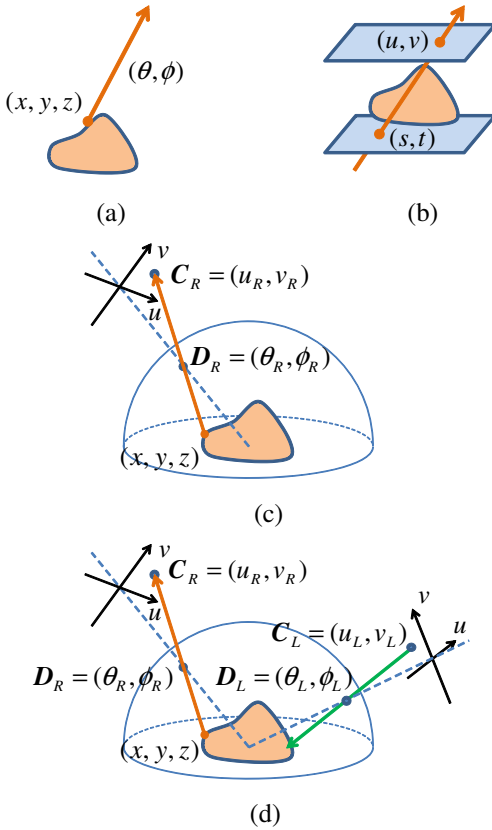


Figure 1. Descriptions of the light and reflectance fields. Both illumination and reflection can be described as a 4DLF. Hence the combination can be represented as an 8DRF.

consisting of the two 4DLFs of illumination and reflection. This eight dimensional reflectance field (8DRF) can perfectly describe the image of the scene from arbitrary view points under arbitrary illumination conditions.

2.2. Measuring device of the reflectance field

Unfortunately, it is difficult to densely measure an eight dimensional reflectance field (8DRF) because of its high dimensionality. To measure the whole 8DRF, many cameras and projectors need to be densely placed around the target. Hence, conventional approaches have restricted the dimensionality[4][5][8] or the spatial area[3][1].

To overcome this problem, we have developed a measuring device for the 8DRF located at uniform intervals on a hemisphere[7]. The core optical device is a polyhedral mirror called the *turtleback reflector*, which locates many virtual cameras and projectors on a hemisphere covering the target scene. The system design and the sample image captured by the measuring device are

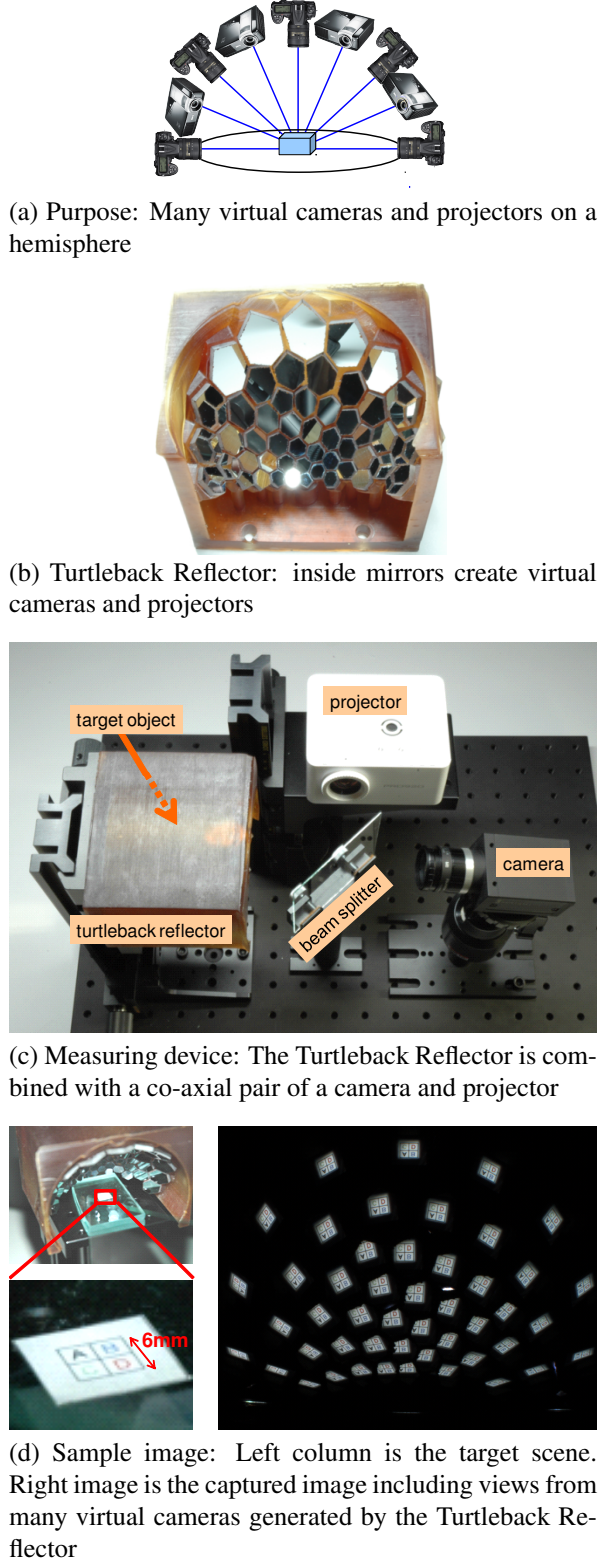


Figure 2. Measuring device for the 8DRF[7].

shown in Fig.2.

3. Computational photography techniques

In this section, we formulate some computational photography techniques for the computation of an 8DRF in a unified framework. We unify the synthetic aperture, image-based relighting, and confocal imaging.

3.1. Synthetic aperture

The synthetic aperture technique[9] realizes a virtual shallow depth-of-field (DoF). The imaging technique accumulates aligned multi-viewpoint images captured by a shifting camera or a camera array. Since the focal depth can be adaptively shifted by changing the aligned position, it is useful for refocusing.

The synthetic aperture can be formulated as a computation of an 8DRF. We synthesize an aperture A centered at D_R as shown in Fig.3. The focal plane is defined as a surface Π . The focused point S is derived by the intersection of the focal plane Π and a viewing ray passing through D_R along C_R . The mask function M , whether or not a ray passes through the point S and the aperture A :

$$M(D, C, S, A) = \begin{cases} 1: & \text{if the ray passes } S \text{ and } D \in A \\ 0: & \text{otherwise.} \end{cases} \quad (2)$$

The synthetic aperture imaging can be represented by an integration of the eight dimensional reflectance field F with the mask function over the hemisphere. The following expression derives the intensity I of a pixel C_R on the image captured by a virtual camera with the aperture A and viewpoint D_R :

$$I(D_R, C_R, A, \Pi) = \iiint F(D_L, C_L, D'_R, C'_R) \cdot F_L(D_L, C_L) \cdot M(D'_R, C'_R, S, A) \cdot dD_L dC_L dD'_R dC'_R, \quad (3)$$

where S is a function of D_R , C_R and Π . F_L is given as a constant 4DLF of illumination.

Figure 4 shows the result of the synthetic aperture on our framework using our 8DRF measuring device. This imaging technique synthesizes the shallow DoF images. The experimental scene consists of the textured transparent sheet over the textured paper as shown in (a). Since the gap between the two layers is only 1 mm, the two textures are mixed if a normal camera is used as shown in (b). The images (c) and (d) are the results of refocusing on the sheet and the paper. We can see that two layers are well separated. This confirms the synthetic aperture is successfully accomplished using the 8DRF measuring device.

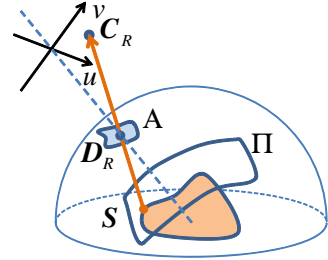


Figure 3. Synthetic aperture. This is achieved by an accumulation of intensities of rays passing through an aperture to make a target focal plane.

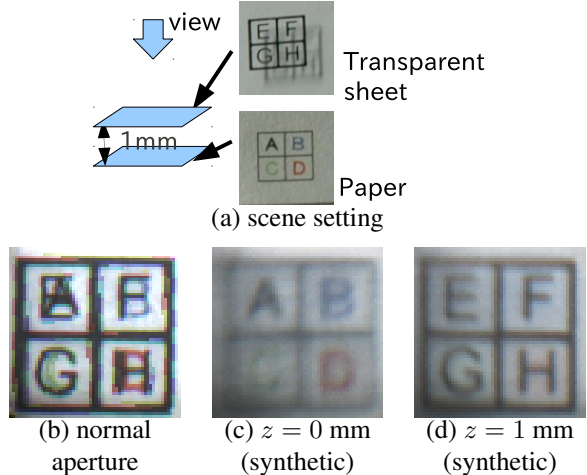


Figure 4. The results of the synthetic aperture. The scene consists of a textured transparent sheet and textured paper beneath the sheet. In the normal aperture image, both the textures are mixed. In the synthetic images, the textures are separately focused and can be read.

3.2. Image-based relighting

The image-based relighting technique can generate a realistic image of a scene under arbitrary illumination[2]. The technique is achieved using a simple combination of the captured images under different illuminations.

This technique is also formulated on an 8DRF. Illumination of the scene is completely described by a four dimensional illumination light field F_L . For a camera fixed at D_R , as shown in Fig.5, the intensity I of the pixel C_R of the camera image can be expressed as:

$$I(D_R, C_R, F_L) = \iint F(D_L, C_L, D_R, C_R) \cdot F_L(D_L, C_L) dD_L dC_L. \quad (4)$$

The F_L can be given arbitrarily.

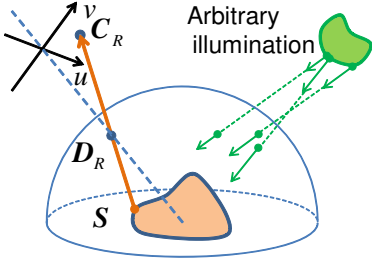


Figure 5. Image-based relighting. Given the illumination condition, the images can be synthesized from the corresponding observations in the 8DRF.

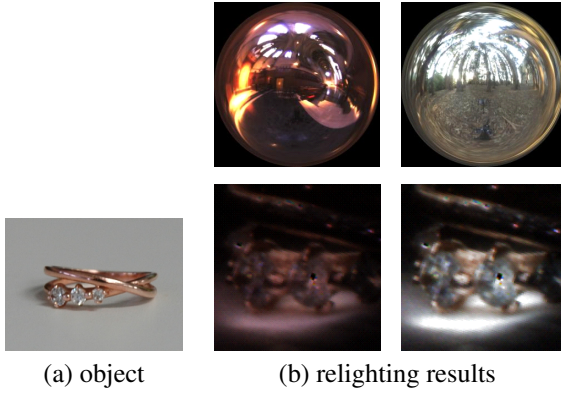


Figure 6. The results of the image-based relighting. For the given illuminations (top row), the corresponding appearances can be reproduced by simple computation of the 8DRF (bottom row).

Figure 6 shows the results of the image-based relighting on our framework using the 8DRF measuring device. The target object is a metallic ring (a) which has complex reflectance properties. In general, it is difficult to synthesize a realistic view under arbitrary illumination by modeling the reflectance. The top row of (b) shows the illumination conditions¹. Fifty pixel values were sampled for illumination because the used device has fifty light sources. The bottom row shows the synthesized images corresponding to the illumination conditions approximately generated by fifty point light sources.

3.3. Confocal imaging

The confocal imaging technique is used in microscopy. It can clearly create an image at the depth of interest by simultaneously scanning the illumination and observation using a pinhole.

The confocal imaging can be formulated as a com-

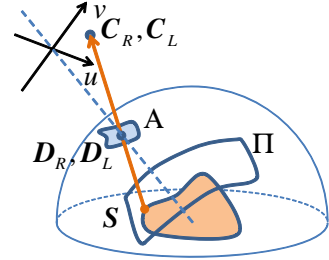


Figure 7. Confocal imaging. The observation and illumination have the same focal plane.

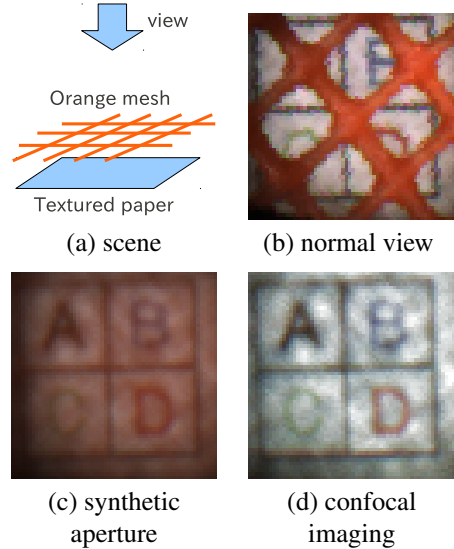


Figure 8. The result of confocal imaging. The scene consists of the textured paper and overlapped orange mesh. In the normal view, the textured paper is partially occluded by the mesh. In the synthetic aperture image, the texture is recognizable because the mesh is significantly blurred, while the orange color remains. In the confocal image, the texture becomes clear because the mesh is significantly blurred and less illuminated.

putation of an 8DRF because an 8DRF can synthesize a large aperture for both illumination and observation. Scanning a pinhole synthesizes a virtual aperture A at the center point D on a hemispherical surface. The target focal surface in the scene is given as Π .

The mask function M indicates whether the ray from a focused point S on the focal plane Π passes through the aperture A as shown in Fig.7.

$$M(D, C, S, A) = \begin{cases} 1 & \text{if the ray passes } S \text{ and } D \in A \\ 0 & \text{otherwise} \end{cases} \quad (5)$$

The confocal imaging can be represented by an integra-

¹The images areDebevec's light probe images at <http://ict.debevec.org/~debevec/Probes/>

tion of the 8DRF with the mask function. The following expression derives the intensity I of a pixel C_R on the image captured by a virtual aperture A for both illumination and observation and the viewpoint D_R :

$$I(D_R, C_R, A, \Pi) = \iiint F(D_L, C_L, D'_R, C'_R) \cdot M(D_L, C_L, S, A) \cdot M(D'_R, C'_R, S, A) \cdot dD_L dC_L dD'_R dC'_R \quad (6)$$

Figure 8 shows the result of the confocal imaging on our framework using the 8DRF measuring device. The target scene consists of the target textured paper beneath an occluding orange mesh as shown in (a). In a view captured by a normal camera, the orange mesh occludes the texture as in (b). Although, as shown in (c), the synthetic aperture can blur the mesh, the texture is still unclear. The result of confocal imaging presents clear texture of the paper and less effect from the mesh as shown in (d).

4. Conclusions

We have proposed a novel framework to express computational photography techniques on an 8DRF. As far as we know, there is no research explaining the relationship between the computational photography techniques and the 8DRF, because there is no real device that can measure an 8DRF.

Recently, we developed a unique device which can sample an 8DRF with uniform angular intervals on a hemisphere. This paper shows that different types of computational photography techniques can be realized by an 8DRF measuring device in the proposed framework.

We expect other computational photography techniques can be explained by the framework, and can be easily implemented using an 8DRF measurement device in the framework. We believe the framework inspires novel computational photography techniques.

Acknowledgement

This research is granted by the Japan Society for the Promotion of Science (JSPS) through the “Funding Program for Next Generation World-Leading Researchers (NEXT Program),” initiated by the Council for Science and Technology Policy (CSTP).

References

- [1] O. Cossairt, S. K. Nayar, and R. Ramamoorthi. Light field transfer: Global illumination between real and synthetic objects. *Proc. SIGGRAPH2008*, pages 1–6, 2008.
- [2] P.Debevec, T. Hawkins, C. Tchou, H.-P. Duiker, W. Sarokin, and M. Sagar. Acquiring the reflectance field of a human face. *Proc. SIGGRAPH2000*, pages 145–156, 2000.
- [3] M. Levoy, B. Chen, V. Vaish, M. Horowitz, I. McDowall, and M. Bolas. Synthetic aperture confocal imaging. *Proc. SIGGRAPH2004*, pages 825–834, 2004.
- [4] V. Masselus, P. Peers, P. Dutré, and Y. D. Willems. Relighting with 4d incident light fields. *Proc. SIGGRAPH2003*, pages 613–620, 2003.
- [5] W. Matusik, H. Pfister, A. Ngan, P. Beardsley, R. Ziegler, and L. McMillan. Image-based 3d photography using opacity hulls. *Proc. SIGGRAPH2002*, pages 427–437, 2002.
- [6] M. Minsky. Microscopy apparatus. *US Patent 3013467*, 1961.
- [7] Y. Mukaigawa, S. Tagawa, J. Kim, R. Raskar, Y. Matsushita, and Y. Yagi. Hemispherical confocal imaging using turtleback reflector. *Proc. ACCV2010*, pages 331–344, 2010.
- [8] G. Müller, G. H. Bendels, and R. Klein. Rapid synchronous acquisition of geometry and appearance of cultural heritage artefacts. *Proc. VAST2005*, pages 13–20, 2005.
- [9] V. Vaish, B. Wilburn, N. Joshi, and M. Levoy. Using plane + parallax for calibrate dense camera arrays. *Proc. CVPR 2004*, 2004.